Catalysis Communications 136 (2020) 105922

Contents lists available at ScienceDirect

Catalysis Communications

journal homepage: www.elsevier.com/locate/catcom

Short communication

A novel risedronic acid-modified Nieuwland catalyst for acetylene dimerization

Qixia Zhang[a,1], Congcong Li[a,1], Juan Luo[a], Jianwei Xie[a,b,*], Jinli Zhang[c], Bin Dai[a]

[a] School of Chemistry and Chemical Engineering, Key Laboratory for Green Processing of Chemical Engineering of Xinjiang Bingtuan, Shihezi University, North 4th road, Shihezi 832003, China
[b] College of Chemistry and Bioengineering, Hunan University of Science and Engineering, Yangzitang Road, Yongzhou 425100, China
[c] School of Chemical Engineering and Technology, Tianjin University, Tianjin 300072, China

ARTICLE INFO

Keywords:
Acetylene dimerization
Monovinylacetylene
Cu-based catalyst
Modified Nieuwland catalyst

ABSTRACT

Nieuwland catalyst (NC) was modified with different phosphonic acids ($\mathbf{P_x}$) and evaluated for their acetylene dimerization activity in monovinyl acetylene (MVA) production. Nearly 49.2% of acetylene conversion and 80.3% of MVA selectivity were obtained in 5 mol% risedronic acid ($\mathbf{P_2}$)-modified NC under an acetylene-gas space velocity of 105 h^{-1} at 80 °C, which was 17.8% higher than the yield of the control NC. The characterization results of NC and $\mathbf{P_2}$–NC indicated that the addition of $\mathbf{P_2}$ effectively enhanced the stability of the Cu ions and inhibited oxidation of the active component Cu^+, improving their catalytic activity and long-term stability.

1. Introduction

Chloroprene rubber is a general-purpose polymer material produced by the polymerization of chloroprene (CP). It is an important type of synthetic rubber with broad application prospects [1]. In China, where coal is abundant, CP is mainly produced through C_2H_2-based processes. However, the production efficiency of CP is limited by the dimerization of acetylene to monovinyl acetylene (MVA). The traditional catalyst for acetylene dimerization is the Nieuwland catalyst (NC), invented by Nieuwland in the 1930s, which consists of $CuCl–NH_4Cl–HCl–H_2O$ [2]. This catalyst has always been disadvantaged by low conversion, low selectivity, and high polymer. Therefore, more effective catalysts for acetylene dimerization are urgently required. In recent years, NC have been modified by second metal addition [3–5], ligand modification [6–9], and optimization and intension [10,11]. These modifications have significantly advanced the acetylene dimerization process. However, they also incur drawbacks such as low acetylene conversion and low MVA selectivity.

Phosphonic acids (PAs), a class of organic compounds containing the -$PO(OH)_2$ group, are often used as phosphorus precursors, complexing agents, or catalyst-modifying ligands in the catalysis fields [12–17]. Hao et al. reported an efficient and convenient method for vanillin hydrodeoxygenation using PAs-modified Pd/Al_2O_3 as the catalyst at low temperature. They attributed the improvement to the creation of metal/acid bifunctional sites [12]. Recently, Wang et al. reported that 1-hydroxyethylidene-1,1-diphosphonic acid-modified Cu/activated carbon (AC) catalyst is highly active in acetylene hydrochlorination. This modification boosted the coordination ability of PA and improved the dispersion of active components on the AC support [13]. Kou et al. modified Cu-Zn-Al hydrotalcite-derived oxides with amino trimethylene phosphonic acid (ATMP), and catalytically synthesized isobutanol and ethanol from syngas. The lattice of the CuZnAl-HTDO catalyst is partially destroyed due to the complexation of Cu^{2+} ions with ATMP. It leads to lattice strain and defects, and improves the adsorption and dissociation of CO at the active site of Cu, which accelerates the reaction rate of CO insertion [14]. Zhang et al. modified Au catalysts with etidronic acid and nitrilotri(methylphosphonic acid) for acetylene hydrochlorination. The transfer of electrons from heteroatoms to Au^{n+} due to the coordination of N, P and O, which increases the density of electron clouds around the active center [15]. Although PAs are excellent modifiers or complexing agents in several catalytic reactions, they have rarely been considered in acetylene dimerization.

We have been endeavoring to develop efficient modified NCs for the acetylene dimerization reaction [4,5,7–9]. As part of these efforts, we propose a $\mathbf{P_2}$-modified NC catalyst that converts 49.2% of the C_2H_2 with an MVA selectivity of 80.3%. The effect of $\mathbf{P_2}$ on the microstructure and active components of the catalyst is examined by various techniques:

---

[*] Corresponding author at: School of Chemistry and Chemical Engineering, Key Laboratory for Green Processing of Chemical Engineering of Xinjiang Bingtuan, Shihezi University, North 4th road, Shihezi 832003, China.

E-mail address: cesxjw@foxmail.com (J. Xie).

[1] Equal contribution to this work.

https://doi.org/10.1016/j.catcom.2019.105922
Received 21 October 2019; Received in revised form 13 December 2019; Accepted 24 December 2019

1566-7367/

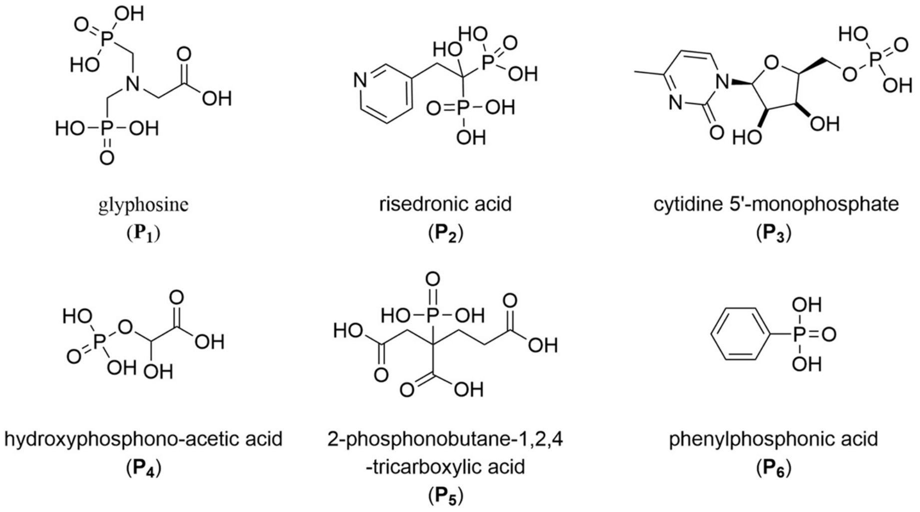

glyphosine (P_1)

risedronic acid (P_2)

cytidine 5'-monophosphate (P_3)

hydroxyphosphono-acetic acid (P_4)

2-phosphonobutane-1,2,4-tricarboxylic acid (P_5)

phenylphosphonic acid (P_6)

Fig. 1. Structures of the six ligands ($\mathbf{P_1}$-$\mathbf{P_6}$).

Fourier-transform infrared spectroscopy (FTIR), X-ray diffraction (XRD), X-ray photoelectron spectroscopy (XPS), thermogravimetry/derivative thermogravimetry (TG/DTG), transmission electron microscopy (TEM), temperature programmed desorption-mass spectrometry (TPD–MS), and inductively coupled plasma (ICP) spectroscopy.

2. Experimental section

2.1. Materials

Glyphosine ($\mathbf{P_1}$), risedronic acid ($\mathbf{P_2}$), cytidine 5′-monophosphate ($\mathbf{P_3}$), hydroxyphosphono-acetic acid ($\mathbf{P_4}$), 2-phosphonobutane-1,2,4-tricarboxylic acid ($\mathbf{P_5}$), phenylphosphonic acid ($\mathbf{P_6}$), CuCl (99%), and NH_4Cl (purity ≥99.5%), were purchased from Adamas and directly used without purification. The molecular structure of the six ligands are shown in Fig. 1. The NCs containing $\mathbf{P_x}$ are denoted as $\mathbf{P_x}$-NC. The amount of $\mathbf{P_x}$ (in moles) was based on the CuCl quantity.

2.2. Catalyst preparation

The catalyst performances were evaluated in a bubble column reactor (length = 400 mm, outer diameter = 40 mm, inner diameter = 10 mm). As a control, an unmodified NC was prepared by dissolving 5.35 g (0.1 mol) of NH_4Cl and 9.9 g (0.1 mol) of CuCl in 10 ml of deionized water at 80 °C. For the experimental specimens, an appropriate molar amount of $\mathbf{P_x}$ (based on the CuCl quantity as mentioned above) was added to the NC. Scheme S1 shows the formation of the gas-phase products in the dimerization process and the catalyst performance evaluation is performed in the C_2H_2 dimerization device (Fig. S1).

2.3. Analytical methods

The criteria of the catalytic performance, namely, the acetylene conversion (X) and MVA selectivity (S), were respectively computed as follows:

$$X = \frac{\lambda_2 + 2\lambda_3 + 2\lambda_4 + 3\lambda_5}{\lambda_1 + \lambda_2 + 2\lambda_3 + 2\lambda_4 + 3\lambda_5} \times 100\%$$

$$S = \frac{2\lambda_3}{\lambda_2 + 2\lambda_3 + 2\lambda_4 + 3\lambda_5} \times 100\%$$

where λ_1, λ_2, λ_3, λ_4, and λ_5 are the volume fractions of the gas products C_2H_2, CH_3CHO, MVA, 2-chloroprene (CP), and divinylacetylene (DVA), respectively.

2.4. Catalyst characterization

The NC and $\mathbf{P_2}$–NC reacted for seven hours were denoted as the used NC and $\mathbf{P_2}$–NC, respectively. The fresh and used NC and $\mathbf{P_2}$–NC were maintained at 3 °C for 6 h in a refrigerator. After cooling, the catalysts were filtered from the catalytic solution, washed with water, and dried in a vacuum oven at 55 °C to obtain a solid catalyst for characterization.

The TG/DTG was performed in a NETZSCH STA 449 F3 Jupiter system (nitrogen atmosphere, temperature range 50–900 °C, ramp rate 10 °C/min). The crystal structures of the samples were determined by XRD ($2\theta = 10$–$90°$). The FT-IR spectra of the catalysts were determined by a Bruker Vertex70 FTIR spectrometer (wavenumber range 500–4000 cm^{-1}). The XPS data was performed in a Kratos AXIS Ultra DLD spectrometer with a monochromatized Al-Kα x-ray source, the deconvolution of the XPS peaks are obtained by the XPSPEAK41 software to process XPS data. The morphologies and microstructures of the samples were recorded by a JEM2100F TEM instrument. The TPD-MS experiments were performed with a Micromeritic ASAP 2720. The absolute Cu contents in the samples were tested by ICP atomic emission spectroscopy (710ES, Varian, USA).

3. Results and discussion

3.1. Catalytic activities of NC and P_x-NC

The performances of the NC and $\mathbf{P_x}$-NCs were initially tested under the same fixed conditions ($T = 80$ °C, C_2H_2 gas hourly space velocity GHSV(C_2H_2) = 105 h^{-1}). The results are shown in Fig. 2. All $\mathbf{P_x}$-NCs exhibited a higher catalytic activity than NC; specifically, the catalytic activity decreased in the order $\mathbf{P_2}$-NC > $\mathbf{P_1}$-NC > $\mathbf{P_6}$-NC > $\mathbf{P_4}$-NC > $\mathbf{P_3}$-NC > $\mathbf{P_5}$-NC > NC. The best performer ($\mathbf{P_2}$-NC) converted 49.2% of the C_2H_2 with an MVA selectivity of 80.3%. The conversion improvement of $\mathbf{P_2}$-NC over NC was 39.5%. Next, we screened the $\mathbf{P_2}$ content (Fig. S2) and the GHSV(C_2H_2) (Fig. S3). The performance was maximized at a $\mathbf{P_2}$ content of 5% ($\mathbf{P_2}$/Cu = 0.05/1). Under a GHSV (C_2H_2) of 80 h^{-1}, the conversion performance improved to 51.1%. In a long-term test, the 5% $\mathbf{P_2}$-NC delivered both excellent activity (51.1% C_2H_2 conversion and 78.8% MVA selectivity) and satisfactory stability (Fig. S4). Therefore, $\mathbf{P_2}$ can significantly enhance the catalytic performance and extend the lifetime of NC for acetylene dimerization.

Contrasting the ligand structure, ligands $\mathbf{P_1}$ and $\mathbf{P_2}$ contain two phosphonic acid groups in six ligands, which may play an important role in high catalytic activity. Phosphonic acid groups are activated by π-electron cloud of benzene, so $\mathbf{P_6}$ has a remarkable effect in the reaction among the $\mathbf{P_3}$-$\mathbf{P_6}$ modified catalysts. By the same way, the

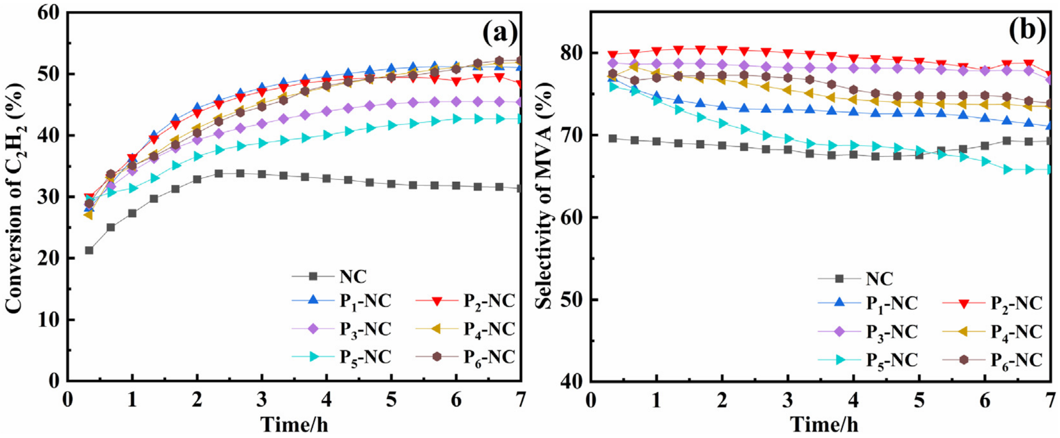

Fig. 2. Catalytic performances of the P_x–NCs ($\mathbf{P_1}$–$\mathbf{P_6}$) on acetylene dimerization: (a) conversion of C_2H_2 and (b) selectivity of MVA. Reaction conditions: $T = 80$ °C, GHSV (C_2H_2) $= 105\ h^{-1}$, $\mathbf{P_x}$ /Cu(I) $= 0.05/1.00$.

pyridine of ligands $\mathbf{P_2}$ may also be an important influencing factor for enhancing catalytic activity. Therefore, it can be concluded that the pyridine and two phosphonic acid groups play an important role in higher catalytic activity of $\mathbf{P_2}$-NC among the modified catalysts.

3.2. *Catalyst characterization*

3.2.1. *Effect of $\mathbf{P_2}$ additive on catalyst appearance*

During the reaction, black solids appeared in the reacting NC and $\mathbf{P_2}$-NC catalysts (Fig. S5), part of the acetylene was polymerized into a high-molecular-weight polymer that adsorbed and encapsulated the active component Cu. Such Cu sequestering is an important cause of catalyst deactivation [3]. Moreover, consistent with the long-term test results, the polymer content was significantly lower in $\mathbf{P_2}$-NC than in NC. The loss of active component was further confirmed by ICP (Table 1).

3.2.2. *Effect of $\mathbf{P_2}$ additive on the catalyst microstructure*

From the HR-TEM analysis, we can see that the major differences between NC and $\mathbf{P_2}$-NC are microstructure of Cu crystal (Fig. S6 a-d) and the irregular conglomerates are Cu crystals. Meanwhile, the microstructure of the fresh $\mathbf{P_2}$–NC revealed many intertwined lamellar crystals. Interestingly, this layer of staggered structures might comprise the active component Cu. Next, it can be found that the high crystallinity and the CuCl single-crystal (Fig. S6 e-h). Typical d-spacing of 0.31 nm and 0.27 nm corresponded to the (111) and (200) planes of the CuCl crystal, respectively. Many CuCl (200) crystal faces (d = 0.26 nm) appear in fresh and used $\mathbf{P_2}$-NC.

The HRTEM images confirm that the $\mathbf{P_2}$ modification changed the crystal morphology. To explore the crystal structure of Cu in the catalyst, the sample was calcined in a tube furnace under a nitrogen atmosphere at 450 °C for 0.5 h. Fig. 3 shows the XRD patterns of the fresh and used NC and $\mathbf{P_2}$-NC after calcination. The diffraction peaks at 28.5°, 33.0°, 47.4°, 56.3°, 69.3°, 76.5°, and 88.3° correspond to the (111), (200), (220), (311), (400), (331) and (422) crystal faces of CuCl, respectively [18]. The spectrum of the fresh $\mathbf{P_2}$-NC reveals additional peaks at 43.3°, 50.4°, and 74.1°, which are contributed by the (111), (200) and (220) crystal faces of Cu, respectively. These peaks are not obvious in the spectrum of the used $\mathbf{P_2}$-NC, implying that Cu^+ was reduced to Cu^0 when the ligand $\mathbf{P_2}$ interacted with Cu^+ during the catalyst preparation, and that Cu^0 was oxidized to Cu^+ after seven hours of the reaction.

Table 1
Relative contents and binding energies of $Cu^{\ +}$ and $Cu^{2\ +}$ in the four samples, determined by XPS and ICP.

Sample	Composition (%)[a]		Cu% (Metal ion content)[b]	Cu loss (%)
	Cu^+	Cu^{2+}		
Fresh NC	72.48	27.52	42.08	16.90
Used NC	62.76	37.24	34.97	
Fresh $\mathbf{P_2}$-NC	80.97	19.03	42.9	5.48
Used $\mathbf{P_2}$-NC	72.96	27.04	40.53	

[a] Determined by XPS.

[b] Determined by ICP.

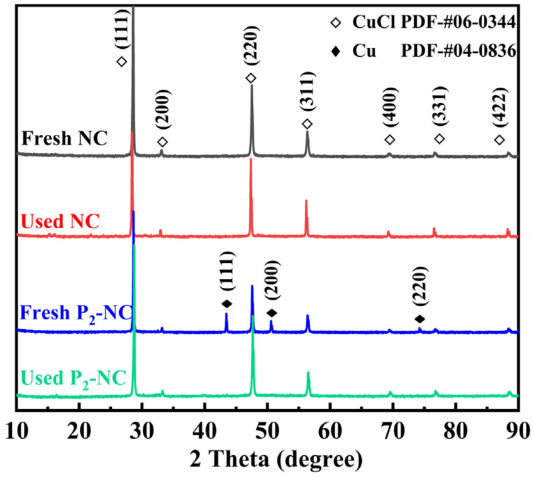

Fig. 3. XRD spectra of the fresh and used NCs and P2–NCs after calcination.

3.2.3. *Coordination between the active components and functional groups of $\mathbf{P_2}$*

Fig. 4 shows the FT-IR spectra of the fresh NCs and $\mathbf{P_2}$–NCs. The absorption peak at 3164.52 cm^{-1} in the fresh NC is the OH stretching vibration induced by chemisorbed water, adsorbed copper hydroxyl groups, and aqua complexes [19]. In the fresh $\mathbf{P_2}$-NC spectrum, the peak attributable to O—H telescopic vibrations is blue shifted by 3.57 cm^{-1} relative to the NC peak, and the absorption peak at 1300–900 cm^{-1} may be contributed by phosphorus-containing groups (P═O and P–OH) [20]. The latter peak would form if the phosphorus-containing group in the ligand were coordinated with Cu in the fresh $\mathbf{P_2}$-NC.

Fig. S7 shows the FT-IR spectra of all catalysts, which can be further explored the effect of functional groups on the catalyst. Obviously, the peaks of phosphorus-containing groups (1300–900 cm^{-1}) appears in

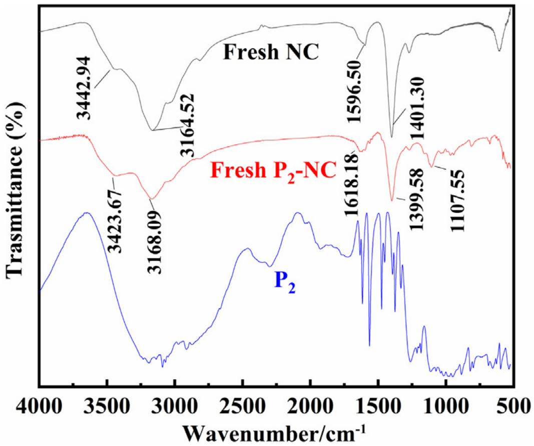

Fig. 4. FTIR spectra of the fresh NCs and P2–NCs.

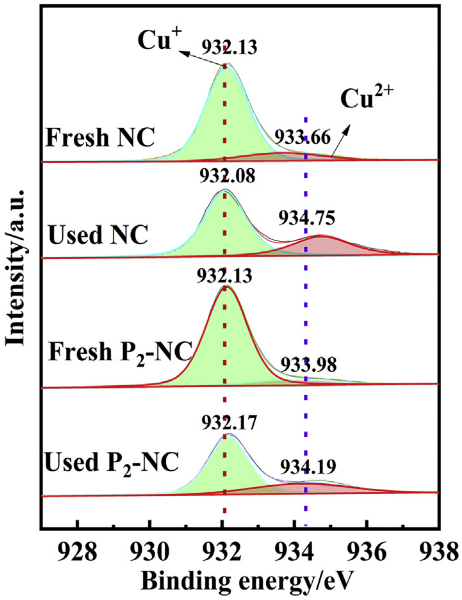

Fig. 5. XPS spectra of Cu 2p3/2 in the fresh and used catalysts.

the FT-IR spectra of the fresh $\mathbf{P_1}$-NC, $\mathbf{P_2}$-NC and $\mathbf{P_6}$-NC. In the fresh $\mathbf{P_2}$-NC, the larger peaks at 1300–900 cm^{-1} is higher than other catalysts, which proves that the coordination ability between Cu and $\mathbf{P_2}$ is stronger than other catalysts. Combined with the results of the catalytic activity, it can be further confirmed that the pyridine and two phosphonic acid groups play a vital role in higher catalytic activity of the $\mathbf{P_2}$-NC among the modified catalysts.

3.2.4. *Role of coordination between the catalyst and* $\mathbf{P_2}$ *(determined by TG/DTG analysis)*

From the TG/DTG analysis, we see that the major differences between NC and $\mathbf{P_2}$–NC are temperature range of the third mass loss (Fig. S8 and Table S1). The temperature of the first mass loss, attributable to the quality loss of crystal water [8,9], was approximately the same in both NC. This result was confirmed by FT-IR analysis of the catalysts containing crystal water. In the case of fresh NC and $\mathbf{P_2}$-NC, the second stage included the loss of NH_3 [21]. In contrast, the temperature of the final mass loss, which mainly reflected the loss of CuCl, greatly different between the fresh NC and fresh $\mathbf{P_2}$-NC (463–700 °C *vs* 543–818 °C). This difference probably caused by the coordination effect between copper and $\mathbf{P_2}$. In addition, all modified catalysts were characterized by TG/DTG (**Fig. S9**), which shown the temperature of the final mass loss in fresh $\mathbf{P_2}$–NC was higher than other modified catalysts. It is inferred that the coordination between Cu and $\mathbf{P_2}$ enhances the thermal stability of the Cu ions.

3.2.5. *Valence changes in the active species*

The XPS analysis provides the chemical state and distribution of the active component Cu in the catalyst before and after the reaction. The XPS peaks at 932.13 and 933.66 eV in Fig. 5 are derived from Cu^+ and Cu^{2+}, respectively [8,9,13]. Table 1 lists the relative Cu^{2+} and Cu^+ contents in the NC catalysts, derived from the relative areas of their XPS peaks. The relative Cu^+ contents were 72.48% and 80.97% respectively in the fresh NC and $\mathbf{P_2}$–NC, and 62.76% and 72.96% respectively in the used NC and $\mathbf{P_2}$–NC. In the $\mathbf{P_2}$–NC, the $\mathbf{P_2}$ reduction induced the partial reduction of Cu^{2+} to Cu^+, confirming that the Cu^0 in the XRD analysis (Fig. 3) was contributed by the reduction of $\mathbf{P_2}$. Meanwhile, the Cu contents were 42.08% and 42.9% respectively in the fresh NC and $\mathbf{P_2}$–NC, and 34.97% and 40.53% respectively in the used NC and $\mathbf{P_2}$–NC. This implies that the Cu-ion loss was much lower in $\mathbf{P_2}$–NC than in NC; that is, the $\mathbf{P_2}$ additive effectively inhibited the loss of Cu ions from the catalyst.

4. Conclusions

An NC system was modified with risedronic acid ($\mathbf{P_2}$) to accelerate the acetylene dimerization reaction. At the optimized $\mathbf{P_2}$ concentration (5%), the $\mathbf{P_2}$-NC was stable and achieved an acetylene conversion of 49.2% with an MVA selectivity of 80.3% under an acetylene GHSV of 105 h^{-1} at 80 °C. The NC and $\mathbf{P_2}$–NC were characterized by FT-IR, HR-TEM, TG/DTG, XPS and ICP. The results indicate that coordination between Cu and $\mathbf{P_2}$ enhances the thermal stability of the Cu ions. During the reaction, the oxidation of the active component Cu^+ is effectively inhibited by $\mathbf{P_2}$. Furthermore, the $\mathbf{P_2}$ additive also inhibits the loss of Cu ions from the catalyst, vitally enhancing the long-term stability of the catalyst. Therefore, $\mathbf{P_2}$ is an excellent phosphorus-containing modifier for NC with high catalytic activity and long-term stability.

Declaration of competing interest

There are no conflicts of interest to declare.

Acknowledgments

We acknowledge the National Natural Science Foundation of China (No. 21776179 and 21463021) for their financial support.

Author Contributions Section

Qixia Zhang: performed the experiments and analyzed the data, wrote the manuscript and supporting information.

Congcong Li: analyzed the data.

Juan Luo: performed the experiments.

Jianwei Xie: designed the project, wrote the manuscript, supervision.

Jinli Zhang: reviewed and edited the manuscript.

Bin Dai: designed the project, reviewed and edited the manuscript.

Declaration of Competing Interests

The authors declare that they have no known competing financial interests or personal relationships that could have appeared to influence the work reported in this paper.

Appendix A. Supplementary data

Supplementary data to this article can be found online at https://

doi.org/10.1016/j.catcom.2019.105922.

References

[1] H. Ismail, H. Leong, Curing characteristics and mechanical properties of natural rubber/chloroprene rubber and epoxidized natural rubber/chloroprene rubber blends, Polym. Test. 20 (2001) 509–516, https://doi.org/10.1016/S0142-9418(00)00067-2.

[2] J.A. Nieuwland, W.S. Calcott, F.B. Downing, A.S. Carter, Acetylene polymers and their derivatives. i. the controlled polymerization of acetylene, J. Am. Chem. Soc. 53 (1931) 4197–4202, https://doi.org/10.1021/ja01362a041.

[3] Z. Liu, Y. Yu, J. Du, X. Fan, C. Tao, Acetylene dimerization catalyzed by $LaCl_3$-modified Nieuwland catalyst, CIESC J. 65 (2014) 1260–1266 (in Chinese), https://doi.org/10.3969/j.issn.0438-1157.2014.04.015.

[4] H. Liu, J. Xie, P. Liu, B. Dai, Effect of Cu^+/Cu^{2+} ratio on the catalytic behavior of anhydrous nieuwland catalyst during dimerization of acetylene, Catalysts 6 (2016) 120–131, https://doi.org/10.3390/catal6080120.

[5] J. Lu, H. Liu, J. Xie, P. Liu, Z. Liu, B. Dai, Study on catalytic activity of zinc (II)-copper(I) collaborative bimetallic catalysis in acetylene dimerization reaction, J. Shihezi Univ. (Nat. Ed.) (2014) 213–217 (in Chinese), 10.13880/j.cnki.65-1174/n.2014.02.017.

[6] R. Chen, G. Deng, R. Mu, G. Liu, Effect of substituted acetic acid ligand on the performance of acetylene dimerization catalyst, Chinese, J. Inorg. Chem. 11 (1995) 89–92 http://en.cnki.com.cn/Article_en/CJFDTotal-WJHX501.016.htm.

[7] J. Lu, H. Liu, J. Xie, P. Liu, B. Dai, Z. Liu, Effect of polyethylene glycol/Nieuwland catalyst on acetylene dimerization reaction, Chem. Eng. 43 (2015) 60–64 (in Chinese), https://doi.org/10.3969/j.issn.1005-9954.2015.06.014.

[8] Y. You, J. Luo, J. Xie, B. Dai, Effect of iminodiacetic acid-modified Nieuwland catalyst on the acetylene dimerization reaction, Catalysts 7 (2017) 394–404, https://doi.org/10.3390/catal7120394.

[9] Y. You, J. Luo, J. Xie, J. Zhang, B. Dai, Effects of coordination ability of nitrogen-containing carboxylic acid ligands on Nieuwland catalyst, Catalysts 8 (2018) 337–347, https://doi.org/10.3390/catal8080337.

[10] F. Zhan, W. Huang, External circulating type bubble reactor for acetylene dimerization in synthesis of monovinylcetylene, China Synthetic Rubber Ind. 19 (1996) 214–217 (in Chinese), http://www.cnki.com.cn/Article/CJFDTotal-HCXF604.008.htm.

[11] Q. Zhang, Y. You, J. Xie, B. Dai, J. Zhang, Effect of high-speed shear reactor in liquid phase catalytic reaction of acetylene dimerization, J. Shihezi Univ. (Nat. Edt.) 37 (2019) 67–72 (in Chinese), 10.13880/j.cnki.65-1174/n.2019.01.010.

[12] P. Hao, D.K. Schwartz, J.W. Medlin, Phosphonic acid promotion of supported Pd catalysts for low temperature vanillin hydrodeoxygenation in ethanol, Appl. Catal. A-Gen. 561 (2018) 1–6, https://doi.org/10.1016/j.apcata.2018.05.008.

[13] X. Wang, M. Zhu, B. Dai, Effect of phosphorus ligand on cu-based catalysts for acetylene hydrochlorination, ACS Sustain. Chem. Eng. 7 (2019) 6170–6177, https://doi.org/10.1021/acssuschemeng.8b06379.

[14] J. Kou, S. Cheng, J. Bai, Effects of amino trimethylene phosphonic acid on structure and properties of Cu-Zn-Al hydrotalcite-derived oxides for catalytic synthesis of iso-butanol and ethanol from synthesis gas, Fuel. 255 (2019) 115833, , https://doi.org/10.1016/j.fuel.2019.115833.

[15] C. Zhang, H. Zhang, Y. Li, L. Xu, J. Li, L. Li, M. Cai, J. Zhang, Hydrochlorination of acetylene over the activated-carbon-supported au catalysts modified by N-P-O-containing ligand, ChemCatChem 11 (2019) 3441–3450, https://doi.org/10.1002/cctc.201900624.

[16] M. Zakeri, E. Abouzari-lotf, M. Miyake, S. Mehdipour-Ataei, K. Shameli, Phosphoric acid functionalized graphene oxide: a highly dispersible carbon-based nanocatalyst for the green synthesis of bio-active pyrazoles, Arab. J. Chem. 12 (2019) 188–197, https://doi.org/10.1016/j.arabjc.2017.11.006.

[17] P.D. Coan, M.B. Griffin, P.N. Ciesielski, J.W. Medlin, Phosphonic acid modifiers for enhancing selective hydrodeoxygenation over Pt catalysts: the role of the catalyst support, J. Catal. 372 (2019) 311–320, https://doi.org/10.1016/j.jcat.2019.03.011.

[18] L. Yang, F. Xiao, Q. Zhang, C. Xu, B. Dai, Non-mercury catalytic acetylene hydration over bimetallic Cu-Zn catalysts for acetaldehyde production in gas-liquid system, ChemistrySelect 4 (2019) 7096–7101, https://doi.org/10.1002/slct.201900954.

[19] S. Biniak, M. Pakuła, G. Szymański, A. Światkowski, Effect of activated carbon surface oxygen-and/or nitrogen-containing groups on adsorption of copper (II) ions from aqueous solution, Langmuir 15 (1999) 6117–6122, https://doi.org/10.1021/la9815704.

[20] D.E.C. Corbrjdge, Infra-red analysis of phosphorus compounds, J. Appl. Chem. 6 (1956) 456–465, https://doi.org/10.1002/jctb.5010061007.

[21] J. Liu, Y. Zuo, M. Han, Z. Wang, Improvement of anhydrous catalyst stability in acetylene dimerization by regulating acidity, J. Chem. Technol. Biot. 88 (2013) 408–414, https://doi.org/10.1002/jctb.3860.